JOURNAL OF AIRCRAFT
Vol. 45, No. 4, July–August 2008

Probabilistic Modeling of Short-Crack Growth in Airframe Aluminum Alloys

Min Liao,* Guillaume Renaud,† and Nick Bellinger‡
National Research Council Canada, Ottawa, Ontario K1A 0R6, Canada

DOI: 10.2514/1.31649

This paper presents a probabilistic short-crack-growth model to estimate the fatigue-life distribution for bare 2024-T351 coupons. Fractographic analysis has clearly shown that the majority of cracks nucleate from the constituent particles present in bare 2024-T351 coupons. The existing fracture mechanics models have difficulty "growing" a small particle-induced crack (i.e., infinite life) and cannot correlate the size of a crack-nucleating particle to the length of the fatigue life in cases in which a small (large) particle results in a short (long) life. In this probabilistic model, particle width and height distributions were first used to account for the randomness of the particle size. Then another random variable, the stress-intensity-factor limit ΔK_{IDS} for particle-induced cracks, was introduced to account for the combined effect of microstructure features (e.g., grain size, grain orientation, and grain boundary) on short-crack growth. A Microsoft Excel Visual Basic for Applications program was developed and linked with the AFGROW component-object-model server to estimate the life distribution using the Monte Carlo technique. The results showed that by including ΔK_{IDS} for particle-induced cracks, the model was able to 1) correlate a crack-nucleating particle to the individual fatigue life, including "smaller (larger) particle, shorter (longer) life" cases, and 2) better estimate the fatigue-life distribution.

Nomenclature

$\mathrm{d}a/\mathrm{d}N$	=	fatigue-crack-growth rate (length per cycle)
H	=	height of a crack-nucleating particle
K	=	stress intensity factor
R	=	stress ratio
W	=	width of a crack-nucleating particle
ΔK	=	stress-intensity-factor range
ΔK_{IDS}	=	stress-intensity-factor limit for an initial-discontinuity-state/particle-induced crack
ΔK_{th}	=	stress-intensity-factor threshold (from a long-crack-growth test)
μ	=	mean of a three-parameter lognormal distribution
σ	=	standard deviation of a three-parameter lognormal distribution
$\sigma_{\max}$	=	maximum stress, ksi
τ	=	threshold (location) of a three-parameter lognormal distribution

I. Introduction

THE National Research Council Canada (NRC) and other organizations are developing the holistic structural integrity process (HOLSIP) to augment and enhance traditional safe-life and damage-tolerance paradigms in both design and sustainment stages. In HOLSIP, the life of a component is divided into four distinct phases: nucleation, short-crack, long-crack, and final-instability [1]. The HOLSIP-based lifing model uses the initial discontinuity state (IDS) as a starting point, which is the intrinsic as-produced or as-manufactured state of a material. Examples of IDS include constituent particles, pores, and machining marks and scratches. All the extrinsic factors, including cyclic and environmental, can modify and interact with the IDS. These interactions can be simulated in the HOLSIP model to assess structural life and residual strength.

One of the major differences between HOLSIP and the historical equivalent initial flaw size (EIFS) lifing models is that the IDS is a physically measured parameter, whereas EIFS is not. The HOLSIP model is physics-based and should be able to correlate IDS with the life of a component, with or without extrinsic effects. So far, the HOLSIP-based models have demonstrated some success in the life estimation of various components, especially in the case of fatigue and corrosion interaction [2–5]. However, due to the complicated physics and the lack of effective experimental techniques and data, many difficulties still exist in the life modeling of the nucleation and short-crack phases. The existing fracture mechanics models have some successes in either estimating the average fatigue life using an EIFS that is close to an average particle size [6] or in estimating the fatigue-life distribution using only the particle distribution at high stress levels [7,8]. But some of the models have difficulty "growing" a small-particle-induced crack (i.e., infinite life), and most of them cannot correlate the size of a crack-nucleating particle to the length of the fatigue life, especially in the cases in which a small (large) particle results in a short (long) life [7,8].

In previous projects, considerable metallurgical studies and coupon fatigue tests were carried out at NRC to physically measure the IDS fatigue subset (i.e., the crack-nucleating constituent particles) for aluminum alloys used in aircraft structures [9,10]. The objectives of the work presented in this paper are to investigate 1) deterministic fracture mechanics models for correlating the crack-nucleating particles with fatigue lives and 2) probabilistic short-crack modeling for estimating fatigue-life distribution.

This paper also presents the results of the investigation on bare 2024-T351 coupons of different thicknesses, subjected to different stress levels (maximum stress and stress ratio) and relative humidity conditions.

Fractographic analysis of bare 2024-T351 sheets has shown that fatigue cracks usually nucleate from the constituent particles, which most have cracked or debonded during the manufacturing (rolling) process. As such, a basic assumption was made that the crack nucleation life is very short or negligible for bare 2024-T351 sheets. The short crack used in this paper refers to the microstructurally short

Presented as Paper 1980 at the 48th AIAA/ASME/ASCE/AHS/ASC Structures, Structural Dynamics, and Materials Conference, Honolulu, HI, 23–26 April 2007; received 16 April 2007; revision received 10 November 2007; accepted for publication 18 December 2007. Copyright © 2008 by the National Research Council of Canada. Published by the American Institute of Aeronautics and Astronautics, Inc., with permission. Copies of this paper may be made for personal or internal use, on condition that the copier pay the $10.00 per-copy fee to the Copyright Clearance Center, Inc., 222 Rosewood Drive, Danvers, MA 01923; include the code 0021-8669/08 $10.00 in correspondence with the CCC.

*Senior Research Officer, Institute for Aerospace Research, Building M14, 1200 Montreal Road. Member AIAA.
†Associate Research Officer, Institute for Aerospace Research, Building M14, 1200 Montreal Road.
‡Group Leader, Senior Research Officer, Institute for Aerospace Research, Building M14, 1200 Montreal Road.

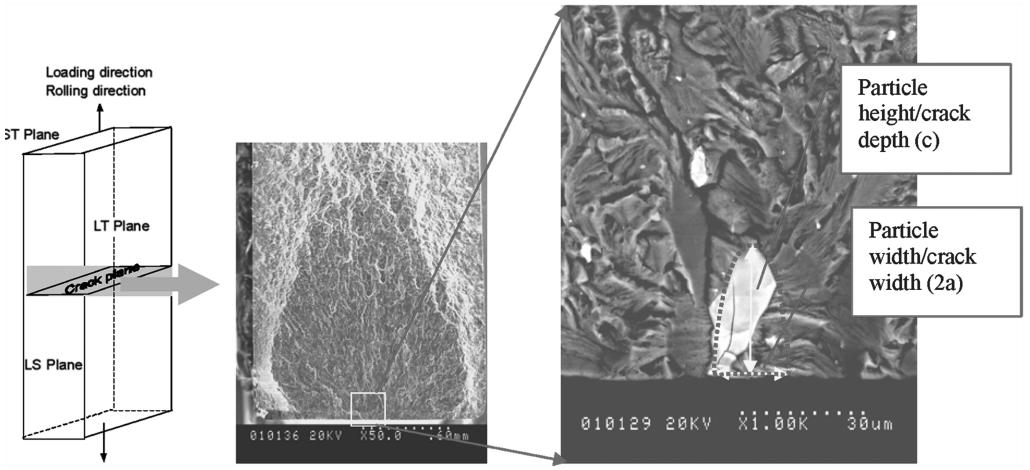

Fig. 1 Fracture surface and crack-nucleating-particle-based crack model (ST denotes the short transverse plane).

crack, for which the growth rate is affected by material microstructures [11,12].

II. Fatigue Tests and Fractographic Analysis

In previous projects, a series of fatigue tests were carried out at NRC using bare 2024-T351 coupons and constant amplitude loading. The complete test conditions for nine groups of fatigue tests are listed in Table 1. The fatigue specimens were hourglass-shaped smooth coupons that were designed based on the American Society for Testing and Materials E466 standards. The specimen orientation with respect to the loading direction is illustrated in Fig. 1. In the fatigue tests, most cracks started from the side surfaces [longitudinal short (LS) plane], some from corners, and only a few from the longitudinal transverse (LT) plane. The fractographic analysis determined that almost all of the cracks nucleated from particles near the surface, and the dominant crack-nucleating particles were measured from the fracture surfaces [9,10], as shown in Fig. 1. In Fig. 2, the crack-nucleating particle sizes vs the number of cycles to failure are shown for groups 1 to 7. An important finding from Fig. 2 is that smaller particles (width and height) could result in shorter fatigue lives, and larger particles could result in longer fatigue lives ["smaller (larger) particle, shorter (longer) life" cases], even under the same test conditions. This kind of correlation cannot be simulated using the conventional fracture mechanics models.

III. Deterministic Fatigue-Life Analysis

As shown in Fig. 1, the crack model used in the life analysis is the semi-elliptical surface crack with dimensions defined by the height and width of the crack-nucleating particle (the IDS/particle-fatigue subset). Although the particle shapes were irregular, a previous finite element study had shown that the maximum stress intensity factor K at the tip of an irregular shape particle was very close to that of a semi-ellipse [13]. In the case in which the true aspect ratio of the crack (or particle width/height) was beyond the limits of the existing K solution, the ratio was set to the limits in the life analysis. This approximation was also demonstrated in [13] and resulted in an accurate K solution.

Because no crack-growth data were collected in the fatigue tests (Table 1), existing material models (i.e., the da/dN–ΔK curve) were used for the life analysis. Several material models for bare 2024-T351 sheets were investigated: the Harter T-model for long cracks in AFGROW, the NASGRO model for long cracks [14], and the modified AGARD-NRC model for short–long cracks [15] (based on the AGARD data in [14]).

After a preliminary analysis, it was found that the Harter T- and NASGRO models gave infinite lives for some coupons presented in Fig. 2 (i.e., a crack would not grow from the measured small particles). This is due to the fairly high stress-intensity-factor threshold ΔK_{th} used in these models, which is usually generated from a long-crack-growth test. The modified AGARD-NRC model was determined using the crack data generated from the AGARD cooperative test program [14]; the high ΔK part (long-crack growth) of the model was taken directly from the AGARD report [14], and the

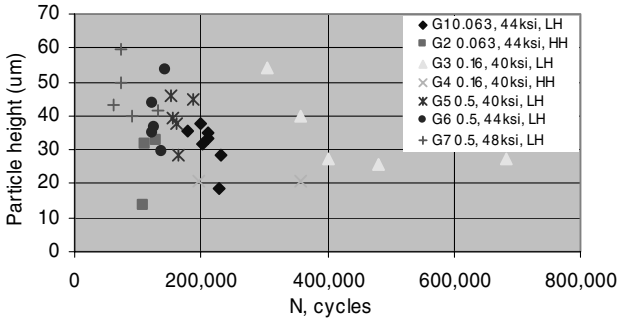

a) Particle height vs cycles

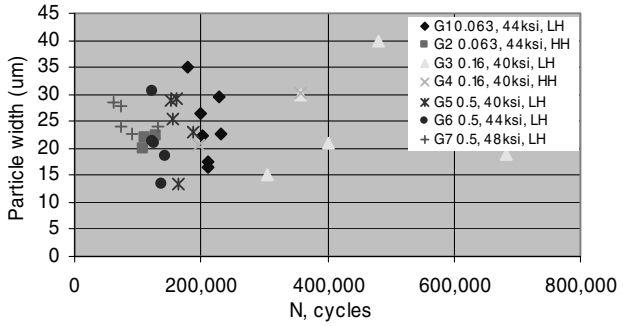

b) Particle width vs cycles

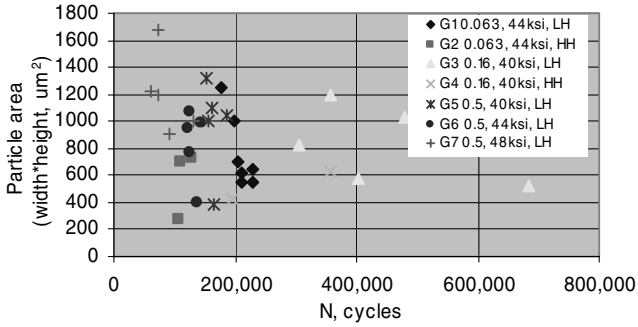

c) Particle area (width*height) vs cycles

Fig. 2 Fatigue test results: crack-nucleating particle size vs number of cycles.

Table 1 Conditions of the fatigue tests

	Group 1	Group 2[a]	Group 3	Group 4[a]	Group 5	Group 6	Group 7	Group 8[b]	Group 9[b]
Stress ratio R	0.1	0.1	0.1	0.1	0.05	0.05	0.05	0.1	0.1
Max. stress, ksi	44	44	40	40	40	44	48	44	48
Relative humidity	Low (less than 2%)	High (98%)	Low (less than 2%)	High (98%)	Low (less than 2%)	Low (less than 2%)	Low (less than 2%)	Low (less than 2%)	Low (less than 2%)
Sample size	7	3	5	5	5	5	5	5	6
Specimen thickness, in.	0.063	0.063	0.16	0.16	0.5	0.5	0.5	0.063	0.063
Specimen min. width, in.	0.375	0.375	0.375	0.375	1.000	1.000	1.000	1.000	1.000

[a]Fatigue lives for groups 2 and 4 tests, which were tested under high humidity, were not used to compare with modeling results in this paper.
[b]Fractographic analysis was not done on groups 8 and 9 specimens, but the fatigue lives were used to compare with the modeling results in this paper.

low ΔK part (short-crack growth) was determined using the limited short-crack data in [14] and a simple extrapolation method [16,17]. After this modification, the model could give finite lives for all of the coupons presented in Fig. 2. Therefore, the modified AGARD-NRC model was applied for further fatigue-life analysis, which is presented in Fig. 3 for three stress ratios, along with the other material models mentioned.

The U.S. Air Force (USAF) crack-growth analysis code AFGROW was used for the life analysis. The modified AGARD-NRC material model was first converted to the tabular lookup format in AFGROW for the required stress ratios R, based on the Walker equation. The tabular lookup data were then used by a Microsoft Excel Visual Basic for Applications (VBA) program to interact with the AFGROW component-object-model (COM) server. The correlation between the test and analytical results is presented in Fig. 4, which indicates that the analytical/test ratio is within the range of 0.4 to 2.5 (a ratio of 1, meaning a perfect correlation). In Fig. 5, the same analytical and test results are presented in an S–N format (maximum stress vs number of cycles). This figure indicates that the scatter in the analytical lives is smaller than that of the tests, especially for the lower stress level (40 ksi). From the deterministic analysis, it is shown that the assumed cracking model and the modified AGARD–NRC material model could provide a reasonably good estimation of the mean of the fatigue lives. However, the life scatter and distribution cannot be calculated by the deterministic approach, nor can the approach model the "smaller (larger) particle, shorter (longer) life" cases found in some fatigue tests.

IV. Probabilistic Modeling of Short-Crack Growth

A. Short-Crack Scatter and Modeling

It is well known that short-crack growth-rate data have more scatter than the long-crack growth-rate data under the same loading conditions. As a typical example, Fig. 6 presents one set of crack data for $R = 0$ and $\sigma_{max} = 145$ MPa, for several specimens, generated by NASA for the AGARD program in 1988 [14] using 2024-T3 single-edge notch-tension specimens. Typical observations are as follows:

There is an *overall* scatter for all the specimens, shown in a scatter band in the figure. This scatter could partially be caused by the differences in specimen geometry, test loading, and measuring technique. Because these extrinsic factors were presumably under control, material intrinsic factors such as particle size, grain size, and grain orientation probably contributed to most of the scatter in the short-crack region.

Each curve shows repeated deceleration and acceleration, especially for very small crack lengths. In addition to the measuring technique, this *individual* deceleration–acceleration behavior can be largely caused by microstructural effects such as the grain-boundary blocking effect, which is associated with the randomness of particle size, grain size, and grain orientation.

From these observations, two probabilistic methods were considered to model the short-crack growth. The first method was still based on fracture mechanics and used random particle size to simulate the *overall* short-crack scatter. The other method was to use random particle size and a grain-boundary barrier model (dislocation-theory-based) to simulate *individual* crack-growth

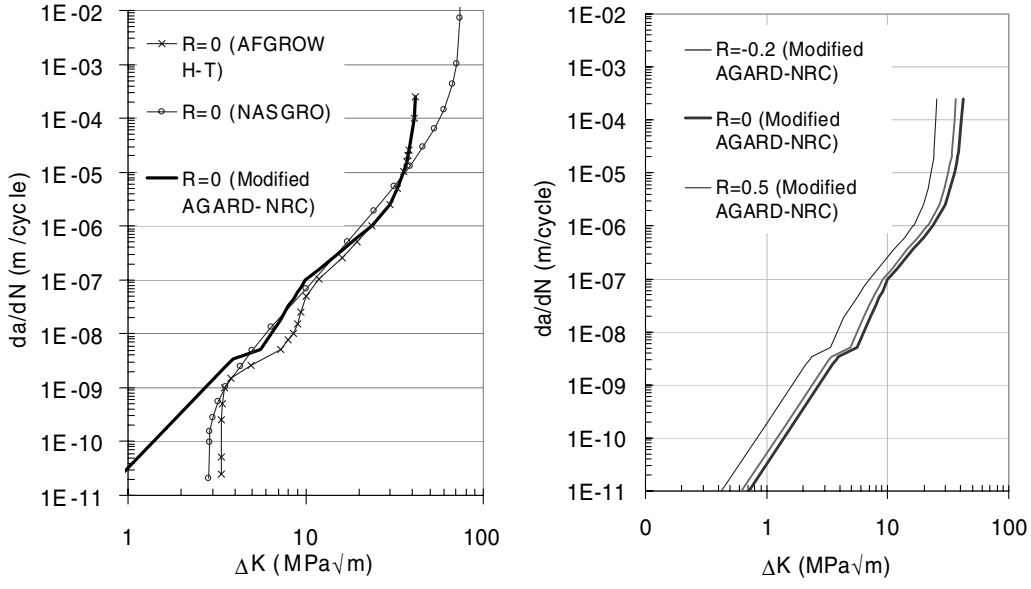

Fig. 3 Material models for bare 2024-T351 sheets from different sources.

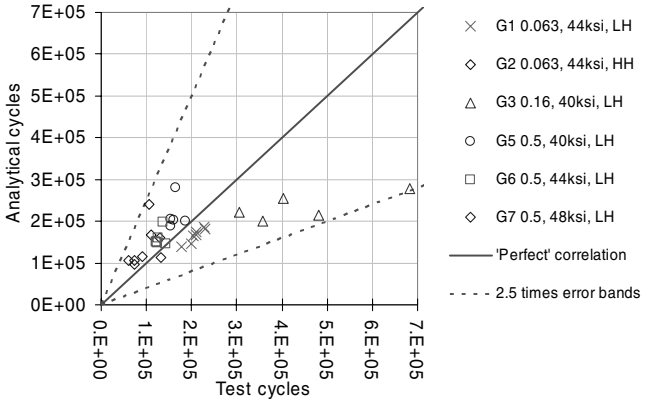

Fig. 4 Correlation between test and analytical lives.

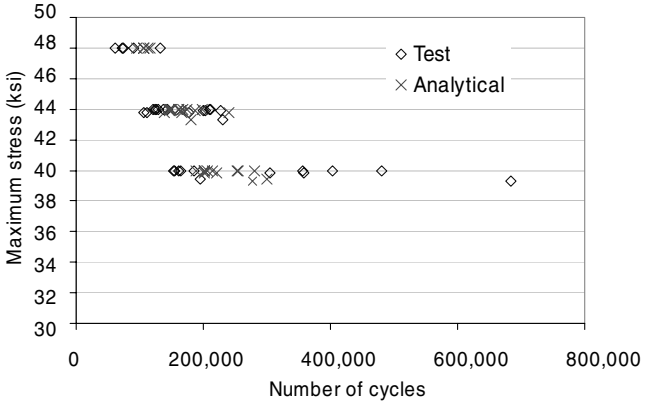

Fig. 5 *S–N* plot of test and analytical results.

behavior as well as the *overall* scatter. Both methods were investigated; this paper presents the modeling efforts using the first method.

B. Probabilistic Short-Crack Model

In the probabilistic model, the crack-nucleating particle width and height were treated as random variables. For a general life-prediction purpose, goodness-of-fit tests were carried out to determine the best-fit distributions for the combined samples for all conditions [18]. Among several distributions, a three-parameter lognormal was found to provide the best fit to the combined samples (particle width and height). Figure 7 presents the distribution fitting to the combined samples, and Table 2 presents the distribution parameters determined by using maximum likelihood methods.

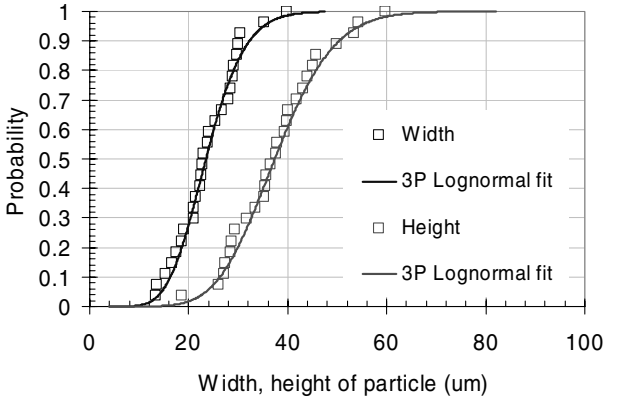

Fig. 7 Distributions of combined particle width and height data (bare 2024-T3; 0.063, 0.16, and 0.5 in. at 40, 44, and 48 ksi; and R0.05, 0.1).

The third random variable was the ΔK limit for the IDS/particle-induced crack, shown in Fig. 1. This ΔK limit is referred to as ΔK_{IDS} in this paper. As in fracture mechanics, ΔK_{IDS} was defined as the limit beyond which cracks can grow at a certain rate from the IDS/particle crack. From the microstructural point of view, ΔK_{IDS} depends on features such as particle size, grain size and orientation, and grain boundary. Considering all the microstructural effects on small-crack growth, ΔK is not necessarily a monotonic function of $\mathrm{d}a/\mathrm{d}N$, because ΔK itself may not be the only driving force in this situation. In this work, ΔK was simplified as a monotonic function of $\mathrm{d}a/\mathrm{d}N$, and a monotonic $\mathrm{d}a/\mathrm{d}N$-vs-ΔK curve was used to represent an average behavior of the repeated deceleration and acceleration behavior exhibited in short-crack growth.

At present, it is impossible to measure ΔK_{IDS} using a conventional crack-growth test, and so a numerical method was developed to estimate its value for each test specimen under the aforementioned assumptions. In this model, ΔK_{IDS} represented the first ΔK value, corresponding to a da/dN of 10^{-11} m/cycle in the modified AGARD–NRC material model. The optimal ΔK_{IDS} was then

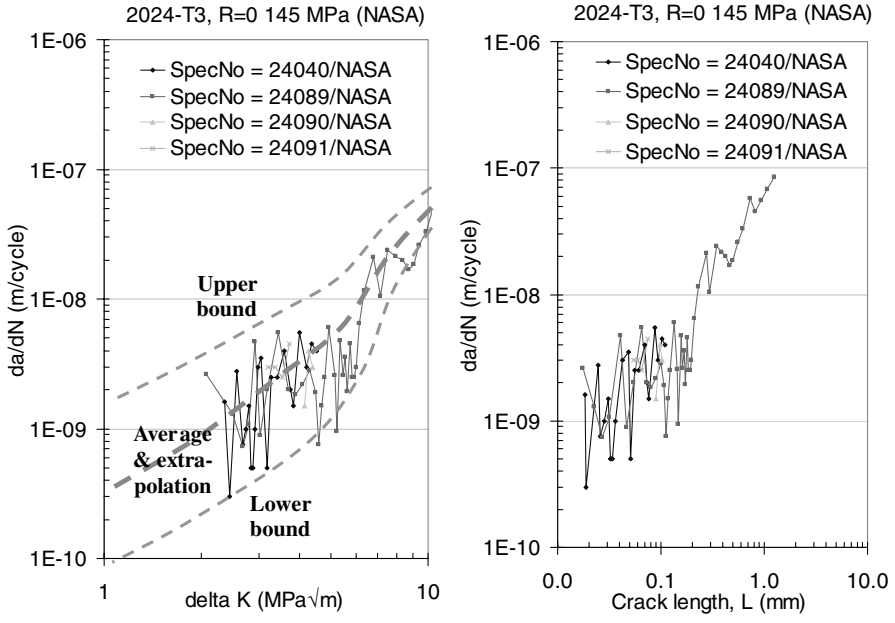

Fig. 6 Small-crack-growth data generated from the NASA/AGARD short-crack program [14]; crack length *L* is the total length of the surface crack in the notch.

Table 2 Distribution parameters of combined particle-size data (2024-T3, bare 0.063, 0.16, and 0.50 in. at 40, 44, 48 ksi, and R0.05, 0.1)

		Particle area, μm^2	Particle width, μm	Particle height, μm
Three-parameter lognormal	Threshold τ	−77.2930	−15.5560	−37.5590
	Mean μ	6.2372	3.6642	4.3166
	Std. dev. σ	0.3386	0.1585	0.1249

determined through an optimization process for each coupon specimen by matching the analytical life to the test. A distribution of ΔK_{IDS} is schematically shown in Fig. 8, along with the modified AGARD-NRC material model and some AGARD data. Note that these AGARD data are presented to show the short-crack behavior and scatter, but may not be the exact data set used for developing the original AGARD material model. A Microsoft Excel VBA program was designed to carry out the optimization, and the analytical results, which were perfectly correlated with the tests, are presented in Fig. 9. A statistical analysis showed that the optimal ΔK_{IDS} values are well-fitted by a truncated normal distribution, as shown in Fig. 10.

It should be noted that by including the third parameter ΔK_{IDS}, the model was able to simulate the "smaller (larger) particle, shorter (longer) life" cases, as shown in Fig. 9. From the microstructural point of view, depending on the surrounding microstructure, a small (large) particle-induced crack may be associated with a small (large) ΔK_{IDS} and may therefore result in a short (long) crack-growth life. Further study on the correlation between particle size (width and height) and the optimal ΔK_{IDS} showed that the correlation was poor.

The probabilistic model was implemented using a Microsoft Excel VBA program, which was developed to run AFGROW using the Monte Carlo technique. The probabilistic life analyses were carried out in different ways by using the following inputs: two random variables (2RV) of particle width and height; two random variables (2RV) of particle width and height with width and height correlated (the correlated random variables were generated using the method in [19], based on the bivariate normal assumption); three random variables (3RV) of particle width, height, and ΔK_{IDS}; three random variables (3RV) of particle width, height, and ΔK_{IDS} with width and height correlated; and three random variables (3RV) of particle width, height, and ΔK_{IDS} with width and ΔK_{IDS} and height and ΔK_{IDS} correlated.

Table 3 presents the analytical results for seven groups of fatigue tests in Table 1, along with the test results. The comparison between the analyses and tests indicate that

1) Both 2RV and 3RV models could give a good estimation of the mean fatigue lives, whereas 3RV models (including ΔK_{IDS}) gave slightly better estimations of the mean.

2) Compared with the 2RV model, the 3RV model resulted in larger standard deviations, which were closer to the tests in some cases, but not in all cases.

3) The correlation between width and height (which was poor) had almost no effect on the mean and standard deviation.

4) The correlations between width and ΔK_{IDS} and between height and ΔK_{IDS} (which were also poor) had little effect on the mean, but decreased the standard deviation.

It should be pointed out that the comparison based on standard deviation is very preliminary, because the test repetition for each group was only five to seven times (see Table 1). To better examine the life-scatter results, the test results listed in Table 1 were regrouped

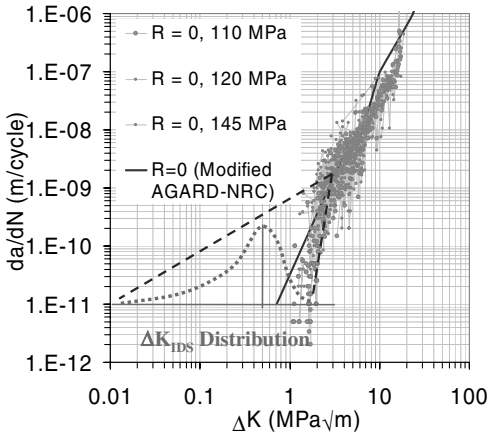

Fig. 8 Schematic of a ΔK_{IDS} distribution with the modified AGARD-NRC model and some AGARD data.

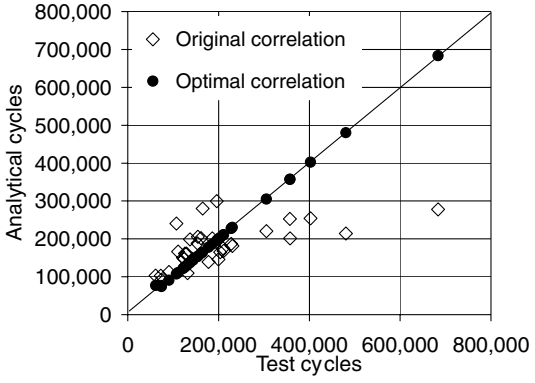

Fig. 9 Optimal analytical and test correlation.

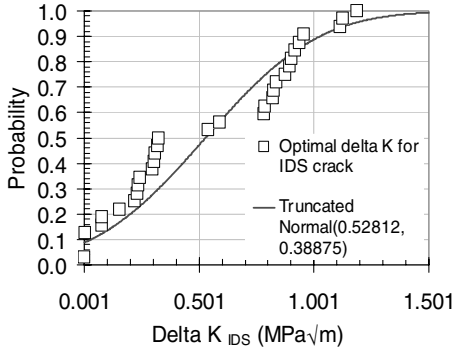

Fig. 10 Optimal ΔK_{IDS} results and the associated distribution.

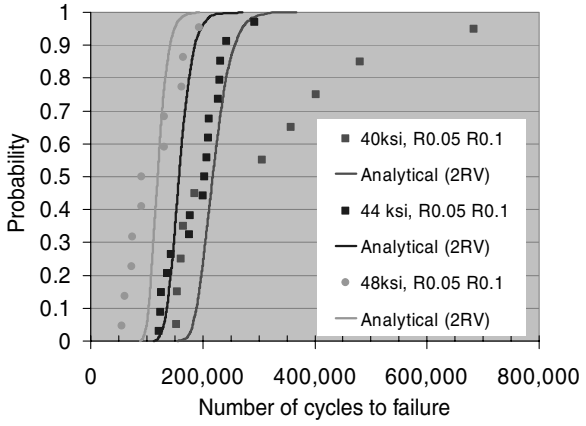

Fig. 11 Probabilistic life modeling using two random variables, particle width and height.

Table 3 Probabilistic fatigue-life analysis and test results

Test groups	Test results[b]		Probabilistic life analysis[a]				
			W, H (independent)	W, H (correlated)	W, H, ΔK_{IDS} (independent)	W, H (correlated), ΔK_{IDS}	W, H, ΔK_{IDS} (correlated)
G1 0.063 in., 44 ksi, R0.1 (CFSD)	Mean	208,558	158,910	158,268	174,232	169,078	164,842
	Std. dev.	17,767	21,237	20,247	87,506	76,556	62,366
	COV	9%	13%	13%	50%	45%	38%
G8 0.063 in., 44 ksi, R0.1 (DUST)	Mean	229,813	158,910	158,268	174,232	169,078	164,842
	Std. dev.	43,086	21,237	20,247	87,506	76,556	62,366
	COV	19%	13%	13%	50%	45%	38%
G9 0.063 in., 48 ksi, R0.1 (DUST)	Mean	133,213	119,862	119,277	124,424	124,562	120,266
	Std. dev.	51,435	15,410	14,504	46,254	45,842	34,596
	COV	39%	13%	12%	37%	37%	29%
G3 0.16 in., 40 ksi, R0.1 (CFSD)	Mean	445,876	222,203	223,162	237,370	243,614	235,848
	Std. dev.	147,652	27,813	27,558	134,558	130,772	109,177
	COV	33%	13%	12%	57%	54%	46%
G5 0.5 in., 40 ksi, R0.05 (DUST)	Mean	164,009	219,031	219,328	231,705	234,266	230,010
	Std. dev.	13,230	26,388	26,413	119,042	117,282	90,761
	COV	8%	12%	12%	51%	50%	39%
G6 0.5 in., 44 ksi, R0.05 (DUST)	Mean	130,531	160,417	160,456	174,356	171,378	165,543
	Std. dev.	9374	19,478	20,925	78,804	78,162	61,221
	COV	7%	12%	13%	45%	46%	37%
G7 0.5 in., 48 ksi, R0.05 (DUST)	Mean	86,151	122,258	121,503	125,651	126,903	123,,654
	Std. dev.	27,537	15,559	14,437	41,361	47,699	33,650
	COV	32%	13%	12%	33%	38%	27%

[a]Monte Carlo AFGROW analysis, the modified AGARD-NRC model, and the listed random variables.
[b]COV is the coefficient of variation.

and combined based on the maximum stress (the difference between the two stress ratios, 0.1 and 0.05, was small and thus ignored). Figures 11 and 12 present the combined test results vs the nonparametric probability determined by the Hazen ranking method; that is, $p_i = (i - 0.5)/n$. The analytical life distributions using the 2RV and 3RV models are also presented in Figs. 11 and 12, respectively. These figures indicate that the 3RV models gave more scattered analytical results, which was more representative of the tests, especially for the lower-stress cases (40 ksi). In addition, Fig. 13 presents the combined analytical and tests results for all stress levels [20]. Overall, the 3RV models performed better than the 2RV models in the life-distribution estimation. In other words, the inclusion of the ΔK_{IDS} distribution in the probabilistic modeling provided a better estimation of the life distribution.

V. Conclusions

A deterministic life analysis was carried out to correlate the measured crack-nucleating particles (IDS/particle-fatigue subset) to the fatigue lives of bare 2024-T351 coupons. It was shown that the modified AGARD-NRC material model could provide reasonably good life estimation. However, the life scatter and distribution could not be calculated using the deterministic approach.

A probabilistic model was developed to estimate the fatigue-life distribution using the Monte Carlo technique implemented by a Microsoft Excel VBA program and AFGROW COM server. Statistical data obtained from various fatigue tests and fractographic analyses were used to address the crack-growth material variability in the short-crack-growth regimes. The comparison between analysis and test results indicated that by using two random variables (i.e., particle width and height), the model could not provide a good

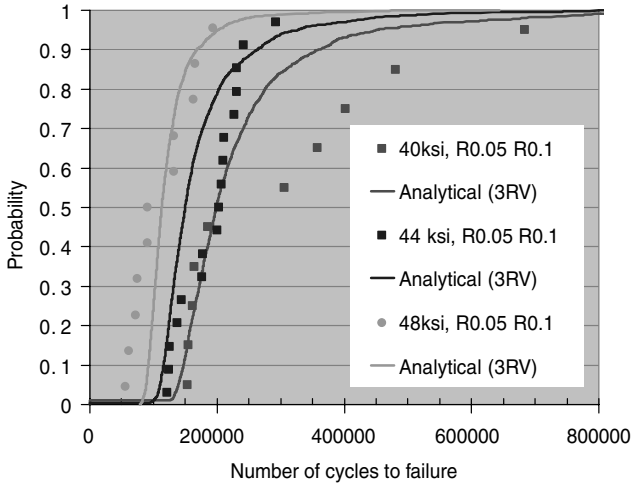

Fig. 12 Probabilistic life modeling using three random variables, particle width, height, and ΔK_{IDS}.

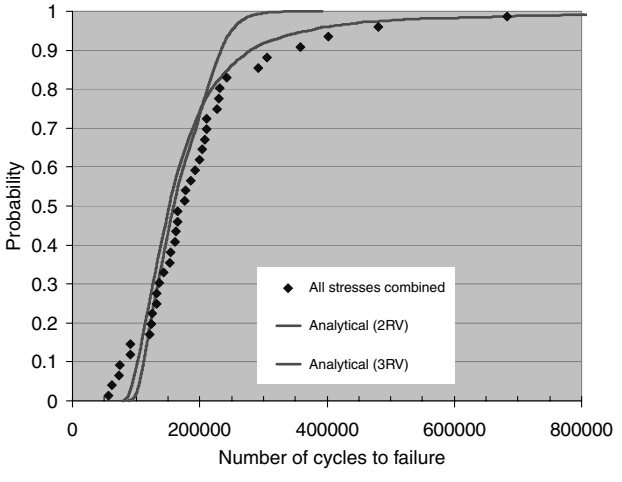

Fig. 13 Combined analytical and test results for all stress levels.

estimation of the life scatter. A fundamental cause is that using only the random particle size in a fracture mechanics model cannot simulate the scatter of short-crack growth, which is also affected by other microstructural features. By including the third random variable ΔK_{IDS} (ΔK limit) for the IDS/particle-induced crack, the presented model could provide a good estimation of the life scatter and distribution. More important, with the parameter ΔK_{IDS}, the model was able to simulate the "smaller (larger) particle, shorter (longer) life" cases found in the tests.

Acknowledgments

This work was carried out with the financial support of the Defence Research and Development Canada (DRDC) and National Research Council Canada (NRC) Short Crack Model Development (46_QJ0_56) and POD and Probabilistic Risk Assessment (46_QJ0_24) projects. The fractorgraphic data were obtained from the previous Corrosion and Fatigue Structure Demonstration project, funded by the U.S. Air Force (USAF), a contract from Lockheed Martin Aeronautics and the Dual Use Science and Technology (DUST) project, partially funded by the USAF through a collaboration with APES Inc.

References

[1] Hoeppner, D. W., "Estimation of Component Life by Application of Fatigue Crack Growth Threshold Knowledge," *Fatigue and Creep of Pressure Vessels for Elevated Temperature Service*, Winter Annual Meeting of the ASME, MPC 17, edited by C. W. Lawton, and R. R. Seeley, American Society of Mechanical Engineers, New York, 1985, pp. 1–85.

[2] Komorowski, J. P., "New Tools for Aircraft Maintenance," *Aircraft Engineering and Aerospace Technology*, Vol. 75, No. 5, 2003, pp. 453–460.

[3] Brooks, C., Honeycutt, K, Prost-Domasky, S., and Peeler, D., "Monitoring the Robustness of Corrosion and Fatigue Prediction Models," *Proceedings of the 2001 USAF ASIP Conference* [CD-ROM], U.S. Air Force, 2001.

[4] Liao, M., Bellinger, N. C., Komorowski, J. P., Rutledge, B., and Hiscocks, R., "Corrosion Fatigue Prediction Using Holistic Life Assessment Methodology," *Fatigue 2002*, Vol. 1, Engineering Materials Advisory Services, Ltd., Heath, England, U.K., June 2002, pp. 691–700.

[5] Liao, M., Bellinger, N. C., and Komorowski, J. P., "A New Probabilistic Damage Tolerance Analysis Tool and Its Application for Corrosion Risk Analysis," *23rd Symposium of the International Committee on Aeronautical Fatigue (ICAF 2005)*, EMAS Publishing, Berlin, June 2005, pp. 241–252.

[6] Newman, J. C., Jr., Phillips, E. P., and Swain, M. H., "Fatigue-Life Prediction Methodology Using Small-Crack Theory," *International Journal of Fatigue*, Vol. 21, No. 2, 1999, pp. 109–119. doi:10.1016/S0142-1123(98)00058-9

[7] Magnusen, P. E., Bucci, R. J., Hinkle, A. J., Brockenbrough, J. R., and Konish, H. J., "Analysis and Prediction of Microstructural Effects on Long-Term Fatigue Performance of an Aluminum Aerospace Alloy," *International Journal of Fatigue*, Vol. 19, No. 93, 1997, pp. 275–283. doi:10.1016/S0142-1123(97)00044-3

[8] Laz, P., "The Influence of Material Variability on Reliable Fatigue Life Predictions in Two Aluminum Alloys," 43rd AIAA/ASME/ASCE/AHS/ASC Structures, Structural Dynamics, and Materials Conference, Denver, CO, AIAA Paper 2002-1379, Apr. 2002.

[9] Merati, A., Tsang, J., and Eastaugh, G.,"Final Report—Test Results for the Determination of Fatigue-Related Features of the Initial Discontinuity State (IDS) of 2024-T3 Aluminum Alloys," National Research Council, TR LTR-SMPL-2003-0001, Ottawa, Ontario, Canada, 2003.

[10] Merati, A., and Awatta, H., "Fractography Results for Fatigue Coupon Testing of Unclad AA2024-T351 Plate," National Research Council, TR LTR-SMPL-2005-0164, Ottawa, Ontario, Canada, 2005.

[11] Suresh, S., *Fatigue of Material*, 2nd ed., Cambridge Univ. Press, New York, 1998.

[12] Miller, K. J., "The Behavior of Short Fatigue Cracks and the Initiation, Part 2: A General Summary," *Fatigue and Fracture of Engineering Materials and Structures*, Vol. 10, No. 2, 1987, pp. 93–113. doi:10.1111/j.1460-2695.1987.tb01153.x

[13] Murakami, Y., Metal Fatigue: Effects of Small Defects and Nonmetallic Inclusions, Elsevier, New York, 2002.

[14] Newman, J. N., "Short-Crack Growth Behavior in an Aluminum Alloy: An AGARD Cooperative Test Programme," NATO/AGARD, Rept. AGARD-R-732, Neuilly-sur-Seine, France, 1988.

[15] Liao, M., and Renaud, G., "A Preliminary Study on Probabilistic Short Crack Modeling for 2024-T351 Aluminum Alloys," National Research Council, TR LTR-SMPL-2006-0007, Ottawa, Ontario, Canada, 2005.

[16] Brooks, C. L., Prost-Domasky, S., and Honeycutt, K., "Determining the Initial Quality State for Materials," *Proceedings of the 2001 USAF ASIP Conference* [CD-ROM], U.S. Air Force, 2001.

[17] Bucci, R. J., Bush, R. W., and Hinkle, A. J., "Aluminum Alloy Forgings Property/Performance Attributes," AGARD Rept. AGARD-AR-353, Neuilly-sur-Seine, France, 1998.

[18] Liao, M., "Statistical Analysis of Constituent Particles of 2024-T351 Aluminum Alloys," National Research Council, TR LTR-IAR-SMPL-2005-0170, Ottawa, Ontario, Canada, Sept. 2005.

[19] Law, A. M., and Kelton, W. D., *Simulation Modeling and Analysis*, 3rd ed., McGraw–Hill, New York, 2000, p. 480.

[20] Renaud, G., and Liao, M., "Probabilistic Modeling of Material Variability in Fatigue Crack Growth," *International Conference on Computer Engineering and Systems (ICCES07)* [online proceedings], Vol. 1, No. 2, http://www.techscience.com/icces/v1n2/ [retrieved 24 Mar. 2008].